SCIENTIFIC FEDERATION
ABODE FOR RESEARCHERS

Anita Grozdanov, SF Nanotec Res Let, 2017, 1:2

SciFed Nanotech Research Letters

Research Article Open Access

Study of Graphene Obtained by Electrolysis in Sulfuric Acid Electrolytes

[1]Aleksandar Petrovski, [1]Aleksandar T. Dimitrov, [*1]Anita Grozdanov, [1]Perica Paunović, [1]Beti Andonović, [2]Gennaro Gentile, [2]Maurizio Avella, [3]Bogdan Ranguelov

[*1]*Faculty of Technology and Metallurgy, University "Sts. Cyril and Methodius" Ruger Bošković Str., 16, 1000 Skopje, R. Macedonia*

[2]*Institute for Polymers, Composites and Biomaterials, National Research Council, Via Campi Flegrei 34, 80078 Pozzuoli, Italy*

[3]*Institute of Physical Chemistry, Bulgarian Academy of Sciences, Acad.G.Bonchev Str., Bl.11, 1113 Sofia, Bulgaria*

Abstract

Last ten years, different methods of graphene production have been developed and reported. The main subject of this work is electrochemical synthesis of graphene using reverse change of the potential. during electrolysis performed in acid electrolyte. As electrodes and precursors for graphene production, two types of graphite were used. Also, three types of electrolytes were used: H_2SO_4 (pH = 0.5); H_2SO_4 + KOH (pH = 1.2) and H_2SO_4 + NaOH (pH = 1.2).

The obtained graphene samples were observed by both, scanning and transmission electron microscope (SEM and TEM). Thermal stability was studied by means of TG, DTG and DTA methods. Different types of bonds were detected by infrared spectroscopy (FTIR). Structural analysis was performed by Raman spectroscopy and X-ray diffraction (XRD). These methods were used for determination of the size of the crystallites and the number of layers of the studied graphene samples. It was found that by the proposed electrochemical method, low-cost, quality and few-layered graphene can be produced.

Keywords

Graphene; Graphene Layers; Crystallite Size; Electrolysis; Reverse Voltage

Introduction

Graphene belongs to graphitic family of nanostructured materials, builded by sp2-bonded carbon atoms packed into a two-dimensional (2D) honeycomb lattice [1, 2]. It completes the order of n-dimensional graphitic materials such as 0D fullerenes, 1D carbon nanotubes, 2D graphene and 3D graphite. It is the basic building unit of all mentioned graphitic materials. Depending on the production procedure, graphene can be produced as a mixture of monolayers, bi-layers and multilayers in form of flakes or flat sheets [3].

The structural arrangement of graphene enables

***Corresponding author:** Anita Grozdanov, Faculty of Technology and Metallurgy, University "Sts. Cyril and Methodius" Ruger Bošković Str., 16, 1000 Skopje, R. Macedonia. E-mail: anita.grozdanov@yahoo.com

Received August 17, 2017; **Accepted** October 24, 2017; **Published** November 8, 2017

Citation: Anita Grozdanov (2017) Study of Graphene Obtained by Electrolysis in Sulfuric Acid Electrolytes. SF Nanotec Res Let 1:2.

Copyright: © 2017 Anita Grozdanov. This is an open-access article distributed under the terms of the Creative Commons Attribution License, which permits unrestricted use, distribution, and reproduction in any medium, provided the original author and source are credited.

remarkable physical properties. So, they show extra-ordinary electrical [4, 5] and thermal conductivity [6], optical transparency [7], mechanical characteristics [8], and highly developed surface area over 2600 $m^2 \bullet g^{-1}$ [9]. As result of these characteristics, graphene is one the most promising nano-scaled material for variety of applications. The unique electrical properties enable wide application of graphene in electronics [10] and optoelectronics (LED screens) [11]. Highly developed surface area and electrical conductivity make graphene an appropriate material for supercapacitors [12], electrocatalysts support and photocatalysts in solar cells [13]. Also, graphene is very promising material for preparation of different types of sensors [14, 15].

Recently, numerous studies were focused on different methods for synthesis of graphene, where very important issues are the product yield and low production costs. Mechanically exfoliated graphene [16] shows excellent properties but this method is not suitable for a high-yield production. Chemical vapor deposition (CVD) [17] offers production of larger quantity of graphene conducting films, but using high-temperatures and expensive catalytic substrates makes this method less cost-effective. Chemical exfoliation covers oxidation of graphite to graphene oxide (GO) and its further chemical or thermal reduction [17, 18]. The disadvantage of this method, however, is an oxidation process which damages the graphene's honeycomb lattices. Also, the high temperature needed for further reduction may cause recover of the graphitic structure. The other methods such as liquid phase exfoliation of graphite [19] or thermal decomposition of a SiC wafer under ultrahigh vacuum conditions [20] are not able to produce the material at a reasonable cost. Many of these methods are followed by disadvantages such as high temperature operations, long time processes (10 hours to days), low-yielded products etc. [21].

Electrolytic exfoliation is an appropriate option for graphene synthesis, offering several advantages over the previously mentioned methods: simple process, reasonable duration, easy controlling (only potential or current regulation), high-yield production, low energy consumption (taking place at room temperature) and environmentally friendly process. Graphene can be produced by two different electrochemical routes [21]. The first one consists of anodic exfoliation of graphite to graphene oxide (GO) and further cathodic reduction of GO to graphene. The second route involves direct cathodic exfoliation of graphene. Electrolytic exfoliation can be performed in both aqueous and non-aqueous electrolytes [21]. Anodic oxidation involves the application of positive potentials to the graphite electrode in order to oxidize it, thereby allowing intercalation of anions leading to structural expansion and ultimate exfoliation of graphene flakes [21]. Graphene oxide (GO) film was evaporated onto graphite and used as an electrode to produce electrochemically reduced graphene oxide (ERGO) films by electrochemical reduction in 6 M KOH solution through voltammetry cycling [22]. Highly efficient and large-scale synthesis of graphene from graphite was produced by electrolytic exfoliation using poly(sodium-4-styrenesulfonate) as an effective electrolyte [23]. Alanyahoğlu and co-workers have studied production of graphene using electrochemical intercalation of sodium dodecyl sulfate (SDS) into graphite followed by electrochemical exfoliation [24]. Average size and thickness of graphene sheets were measured to be about 500 and 1 nm, respectively. Besides the organic solvents as non-aqueous electrolytes, ionic liquids are also used for the electrochemical production of GN flakes. Ionic liquids have the added advantage of being non-volatile and they are also biodegradable [25]. Mostly used aqueous electrolytes are sulfuric [26] and perchloric acids [27].

The aim of this work is to produce high quality graphene using low cost method based on reverse change of the applied potential during electrolysis performed in acid electrolyte. Namely, the novelty of this research work is to present a graphene production method using non-stationary current regimes instead of standard procedure of electrolysis performed by galvanostatic or potentiostatic methods.

2. Experimental

The studied graphene samples were prepared by electrolytic method presented elsewhere [28]. The graphene was exfoliated by intercalation of graphite electrodes (M1 and M2). Electrolysis was performed by reverse change of the applied voltage (+10 to –10 V and +15 V to –15 V). Electrolytes were based on sulfuric acid: pure H_2SO_4 (pH= 0.5), H_2SO_4 + KOH (pH= 1.2) and H_2SO_4 + NaOH (pH= 1.2). The electrolytes were prepared with corresponding chemicals of high purity (p.a.). Before each experiment, the graphite electrodes were pretreated at constant reverse voltage of +5 V to –5 V for 5 minutes. The produced suspension containing graphene sheets was filtered through vacuum filter. Solid phase (graphene sheets) was

repeatedly washed with distillated and deionizated water. The scheme of the experiments is shown in Table 1.

Table 1: Scheme of the Experiments

No of experiment (sample)	Type of graphite	Reverse voltage, V	Electrolyte
1	M1	+10 , –10	H_2SO_4 (pH = 0.5)
2	M1	+10 , –10	H_2SO_4 + KOH (pH = 1.2)
3	M1	+10 , –10	H_2SO_4 + NaOH (pH = 1.2)
4	M1	+15 , –15	H_2SO_4 (pH = 0.5)
5	M1	+15 , –15	H_2SO_4 + KOH (pH = 1.2)
6	M1	+15 , –15	H_2SO_4 + NaOH (pH = 1.2)
7	M2	+10 , –10	H_2SO_4 (pH = 0.5)
8	M2	+10 , –10	H_2SO_4 + KOH (pH = 1.2)
9	M2	+10 , –10	H_2SO_4 + NaOH (pH = 1.2)
10	M2	+15 , –15	H_2SO_4 (pH = 0.5)
11	M2	+15 , –15	H_2SO_4 + KOH (pH = 1.2)
12	M2	+15 , –15	H_2SO_4 + NaOH (pH = 1.2)

Firstly, the produced graphene samples were observed by electron microscopy. Scanning Electron Microscope - JEOL 6390 and Transmission Electrone Microscope FEI Tecnai G2 Spirit TWIN equipped with LaB6 were used. Thermal analysis was performed using Perkin Elmer Pyris Diamond Thermo¬gravi¬metric/Differen¬tial Thermal Analyzer; ATR-FTIR spectroscopy using Perkin Elmer PARAGON system in the region of 400 to 4000 cm^{-1}; X-Ray diffraction using the X-Ray diffractometer type PHILIPS PW3710 (CuKα radiation, λ=1,54056 Å, from 0 to 80 Å).

3. Results and Discussions

3.1 SEM Analysis

SEM analysis was performed in order to make a proper qualitative selection of the produced graphene samples. The obtained SEM photographs of the studied graphene are shown in Figure 1 and Figure 2. Generally, morphological elements of graphene structure were obtained, however with different quality. In Fig. 1a, 1b and 1c, SEM images of graphene produced at reverse voltage of +10 to –10 V from graphite M1 are shown. These samples are characterized with large particles containing lot of defects formed during the exfoliation of graphite. Usually, graphene exhibits very high transparency (97,7%) [29]. However, these images show very low transparency of the produced material indicating higher presence of graphite than graphene. Graphene samples produced in strong acid medium (in pure sulfuric acid (pH = 0.5, Figure 1a)) show large grains (~ 30 μm) with the very low transparency. By adding the alkalis, less damaged material, with smaller dimensions (~10 μm) was obtained (Figure 1b and 1c). The produced material at reverse voltage of 10 V is of poor quality and shows low yield of graphene. The quality of the produced material considerably increases by increasing the working reverse voltage (+15 V to –15 V, see Figure 1d, e and f). The number of defect is decreased, while the transparency is increased (for 70% compared to previous samples). As in the previous samples, addition of alkalis (pH = 1.2) improves the quality of the produced material. Quality improvement of the graphene samples due to the alkalis addition can be achieved because of the lower electrolyte attack (lower acidity), resulting in lower concentration of defects. Also, the exfoliation process can be improved by Na^+ and K^+ ions. Namely, Na+ ions have exhibited better effect than K^+ due to smaller atomic radius (rNa = 186 pm vs. rK = 227 pm). Also, the material produced at voltage of +15 V, has better quality and shows higher yield of graphene. Similar considerations can be drawn for the graphene produced from the second type of graphite M2 (Figure 2). By comparison of both graphene samples exfoliated from the graphite M1 and M2 (Figure 1 and 2), it can be seen that better morphology as well as higher transparency, was found for the samples originated from graphite M2 due to the more oriented structure and better quality of the graphite M2.

Therefore, the samples produced at reverse voltage of +15 to –15 V were selected for further analysis.

Figure 1: SEM Images of Graphene Produced from Graphite M1 at Reverse Voltage; a) RV = +10 to –10 V in H_2SO_4 (pH = 0.5); b) RV = +10 to –10 V in H_2SO_4 + KOH (pH = 1,2); c) RV = +10 to –10 V in H_2SO_4 + NaOH (pH = 1,2); d) RV = +15 to –15 V in H_2SO_4 (pH = 0.5); e) RV = +15 to –15 V in H_2SO_4 + KOH (pH = 1,2); f) RV = +15 to –15 V in H_2SO_4 + NaOH (pH = 1,2)

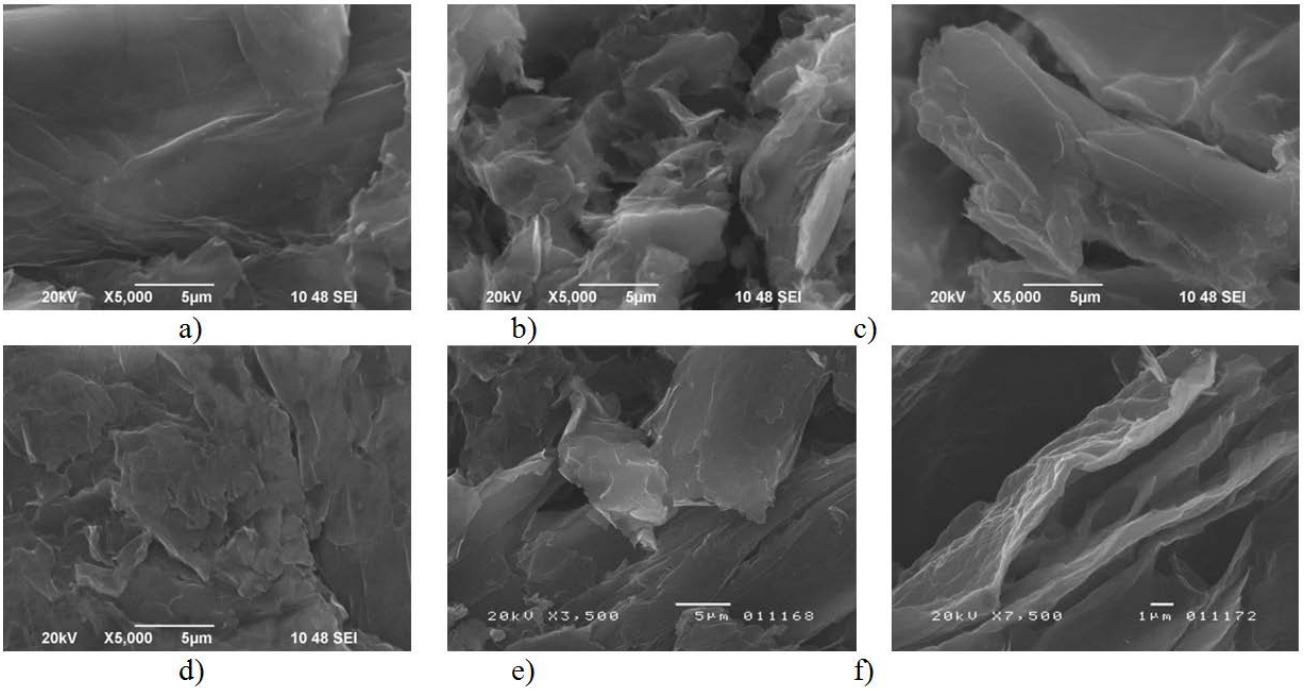

Figure 2: SEM Images of Graphene Produced from Graphite M2 at Reverse Voltage; a) RV = +10 to –10 V in H_2SO_4 (pH = 0.5); b) RV = +10 to –10 V in H_2SO_4 + KOH (pH = 1,2); c) RV = +10 to –10 V in H_2SO_4 + NaOH (pH = 1,2); d) RV = +15 to –15 V in H_2SO_4 (pH = 0.5); e) RV = +15 to –15 V in H_2SO_4 + KOH (pH = 1,2); f) RV = +15 to –15 V in H_2SO_4 + NaOH (pH = 1,2)

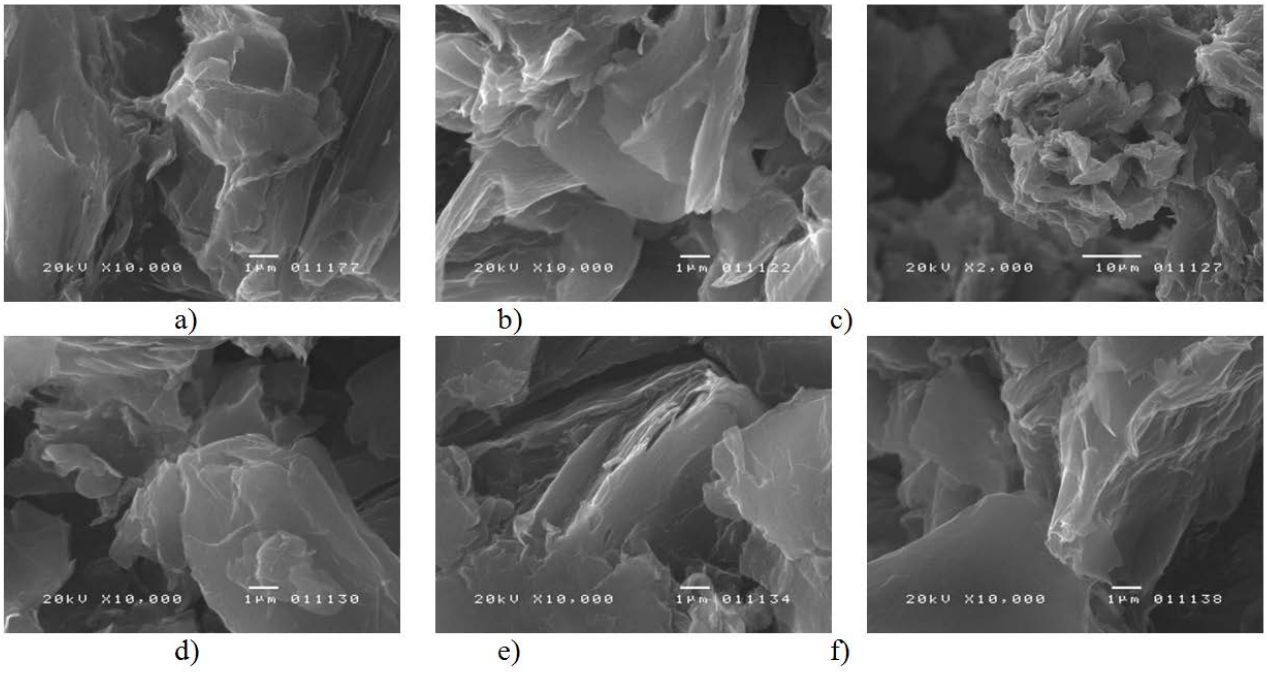

3.2 TEM Analysis

Characteristic photographs of TEM analysis are shown in Figure 3 and Figure 4. Evidently, the observed morphology of the graphene samples produced by reverse electrolysis in aqueous electrolytes corresponding with the morphology of few layers graphene prepared with other methods. Most of the obtained graphene sheets are broken and intertwined. Also, a low amount of impurities, fibers, non-exfoliated graphite and amorphous carbon were found. The sample thickness was determined in the range from few nanometers to 20 nm.

Figure 3: TEM Images of Graphene Produced from Graphite M1 at Reverse Voltage RV = +15 to –15 V in a) H_2SO_4 (pH = 0.5); b) H_2SO_4 + NaOH (pH = 1,2)

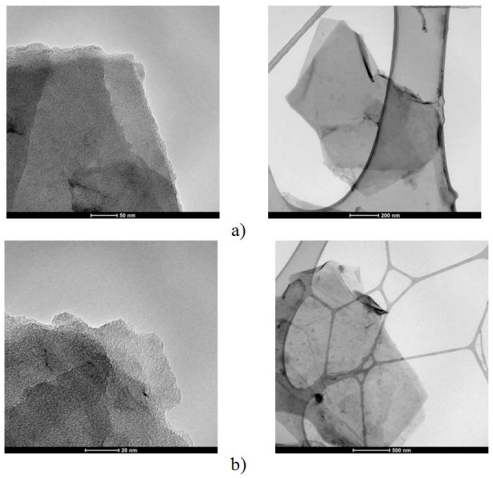

Figure 4: TEM Images of Graphene Produced from Graphite M2 at Reverse Voltage RV = +15 to –15 V in a) H_2SO_4 (pH = 0.5); b) H_2SO_4 + NaOH (pH = 1,2)

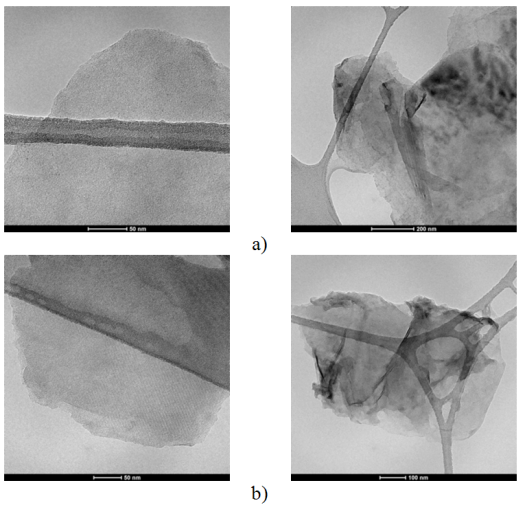

In particular, the best performances (lower thickness and the least number of layers (5-8) were found for the graphene produced from the graphite M2 in sulfuric acid with NaOH. Based on the TEM images, it is evident that the layer number varies in different parts of the sample. So, monolayered, few-layered and multilayered graphene sheets can be observed. These results are in agreement with determination of number of layers obtained by XRD analysis.

3.3 Thermal Analysis

Thermal analysis (TG and DTG) in nitrogen atmosphere was employed to evaluate the thermal stability of the graphene samples. The samples were heated from ambient temperature to 1273,15 K at heating rate of 20 K•min^{-1}. The results are shown in Figure 5. For better elucidation of the results, the characteristic TG and DTG temperatures are shown in Table 2.

Figure 5: Thermal Diagrams of the Studied Graphene Samples: a) TG Curves, b) DTG Curves

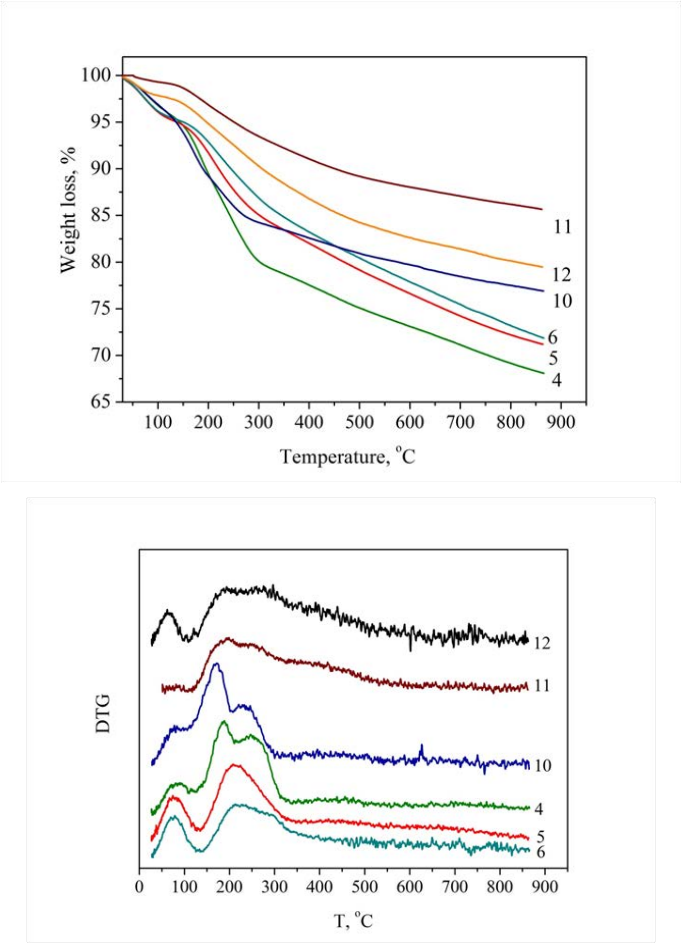

Table 2: Characteristic TG and DTG Temperatures and Mass Losses of the Studied Samples Determined from TG and DTG Spectra Shown in Figure: 5

Sample		TG_1	TG_2	TG_3	TG_4	DTG_1	DTG_2	DTG_3	DTG_4
4	oC	53.1	152.3	375.1	705.5	88.4	190	439	700.7
	wt.%,	98.8	94.3	77.8	70.7				
5	oC	57.3	171.3	415.1		74	208.7	441.6	
	wt.%	99.99	95.8	83					
6	oC	51.1	175			78.6	226.8		
	wt.%	99.99	96.4						
10	oC	53.6	141.5	219.9	395.8	78.4	173.6	228.7	395.4
	wt.%	99.9	94.5	87.5	82.3				
11	oC		145.7			80.9	194.1	255.1	
	wt.%		98.3						
12	oC	61.2	150.2		658	60.9	194.5		736
	wt.%	98.03	96.4		81.2				

The shape of the TG and DTG spectra as well as the characteristic temperatures is in agreement with the literature data [30]. As expected, several mass decreases were registered. First slight mass decrease of 1-2% at TG_1, mainly bellow 373 K, corresponds to dehydration and mass loss of the water humidity. The second, major mass loss at TG_2 (or DTG_2 peak) between 413 to 448 K corresponds to the pyrolysis of oxygen containing functional groups and generates CO and CO_2. The weight loss is only about 2-3.5 % up to 448 K, because most of the functional groups are removed during the reduction. TG_3 corresponds to the oxidation of the sp2-hybridzied carbon atoms (up to 688 K) present in the samples. TG_4 corresponds to the combustion of the graphene and oxidation of the pristine graphite powder occurs above 873 K, usually in the range between 923 and 1033 K. If we compare positions of the characteristic temperatures, samples 4 and 12 show similar structure and thermal behavior versus samples 5 and 10. Since the thermal stability of the obtained graphenes decreases as their thickness decreases, TG results suggest that the samples produced from the graphite M2 have lower thickness (samples 10, 11 and 12) compared to those produced from graphite M1. The sample 4 shows the lowest thickness within the samples produced by graphite M1.

3.4 FTIR-ATR Analysis

The FTIR-ATR spectra (Figure 6) were recorded in the region of 400 to 4000 cm^{-1}. According to the literature, characteristic graphene peaks are registered in the region near 3150 cm^{-1} originated by OH groups, 1300-1650 cm^{-1} originated by C=C bonds and near 1100 cm^{-1} [31].

Figure 6: FTIR Spectra of the Studied Graphene Samples

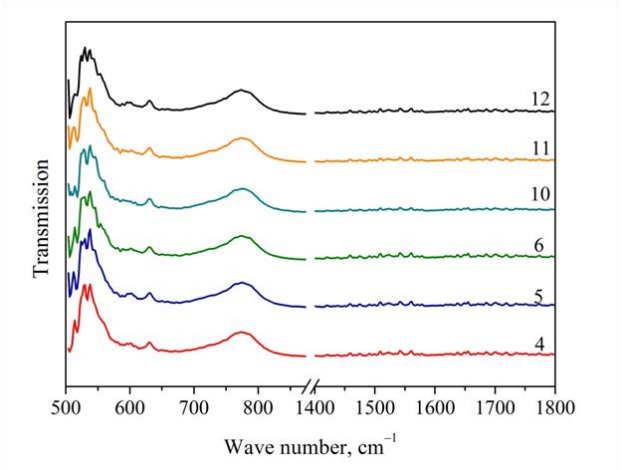

Within the spectra of the studied graphene samples a sharply pronounced peak appears at 772 cm^{-1} as result of C–C bond vibrations which are mostly out of graphene plane (Figure 4). Also, there is change of peaks shape in the region of lower wave numbers (400-525 cm^{-1}). This suggests on C–Cl or C–S bonds originated from chlorine or sulfuric atoms present in the medium in which graphene was produced [32, 33]. In this case it is clear that only C–S bonds are present as result of sulfuric atoms from sulfuric acid.

Analysis of the peak at 772 cm^{-1} for the studied samples indicates change of both its intensity expressed by full width of half maximum (FWHM) and its position

(cm^{-1}). These changes can be attributed to the change of the number of layers which implies on presence of more and different number of layers in different samples [33]. The change of the peak intensities as FWHM for the studied samples is shown in Table 3.

Table 3: Analysis of the Peak Intensity at 772cm^{-1}

Sample	FWHM, cm^{-1}
4	56.8
5	59.9
6	59.2
10	58.9
11	60.4
12	56.8

Determination of FWHM (cm^{-1}) was done by the program GRAMS/386. The lower FWHM points out to more ordered structure of the studied material [32]. Among the samples originated from graphite M1 the most ordered structure shows sample 4 produced in pure sulfuric acid, while between the samples from the second graphite M2 the most ordered structure shows sample 12 produced in the electrolyte containing sulfuric acid and NaOH.

3.5 X-Ray Diffraction Analysis

In order to compare the microstructural parameters of the graphene originated from two graphite forms, M1 and M2, characteristic types of X-Ray diffractograms for sample 4 (from graphite M1) and sample 10 (from graphite M2) were scanned and they are shown in Figure 7. The main peak for both samples appears at position of 2θ= 26,17° which corresponds to diffracting (002) graphite plane (see Table 5). Also, in both samples two broader and less pronounced peaks were registered at position of 2θ= 42.30° and 44.35° corresponding to 100 and 101 reflections. The difference was found in the shape and the full-width at half-peak maximum (FWHM) of the peaks which is closely related to the quantity of well-ordered areas in the structure. More intensive, sharp and narrow peak is obtained for the sample 10 produced from M2 graphite.

Figure 7: XRD Spectra of the Samples 4 and 10

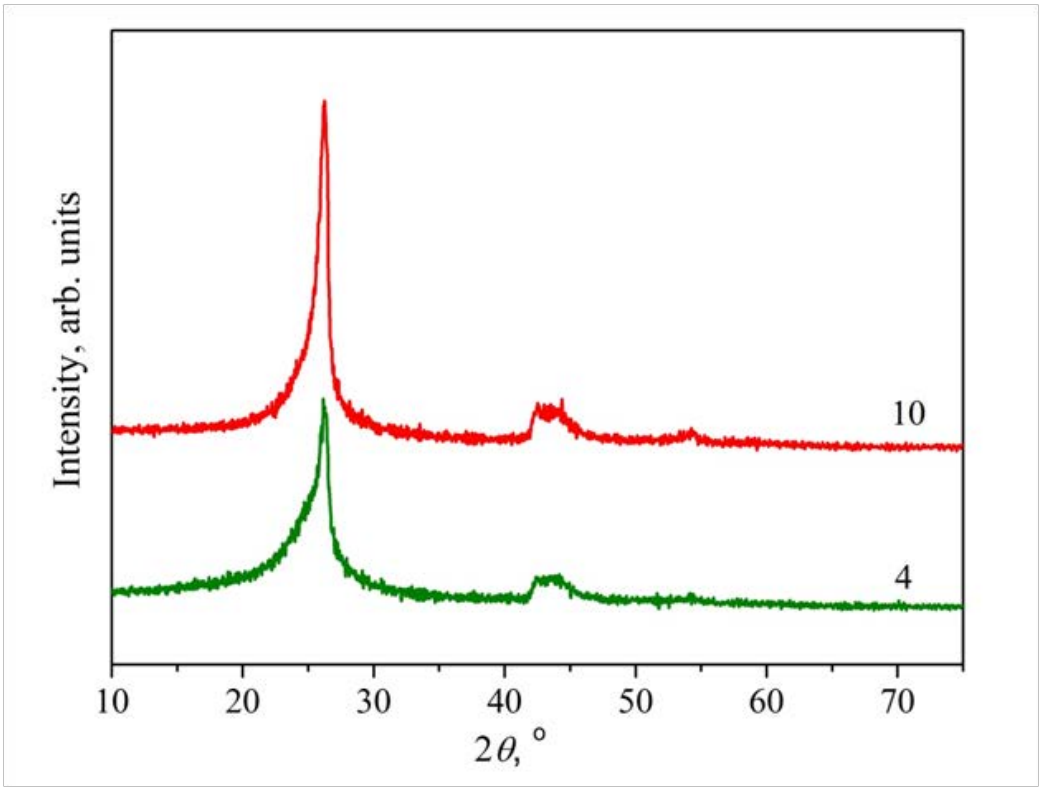

The increase in the intensity of the peak in sample 10 can be attributed to higher X-ray scattering factors [34]. The pronounced (002) peaks at about $2\theta = 26.17^{o}$ were seen (Figure 7) for both samples which are also assigned to the layer-to-layer distance (d-spacing: $d = \lambda / 2\sin\theta$). The crystallites size was evaluated from the width of the diffraction peak using the Scherrer equation $L_a = k \cdot \lambda / \beta \cos\theta$, where k is shape factor; λ is the X-ray wavelength; β is full width at half maximum intensity (FWHM) in radians; θ is the Bragg angle [34]. Characteristic X-ray structural parameters of graphene 4 from M1 and 10 from M2 graphite types are given in the Table 4. The estimated values of L_a are slightly different than corresponding ones estimated by Raman spectra [28], but still in agreement.

Table 4: X-ray Structural Parameters for Graphene 4 and 10 from Plane 002

Sample	2q, plane (002)	FWHM, rad	d, Å	L_a, nm
4	26.12	0.0297	3.4	5.01
10	12.17	0.0384	3.4	3.87

However, more precise determination of the number of graphene layers was done using Laue functions and a model which includes graphene thickness distribution [35, 36]:

$$|F|^2 \sim |f(\theta)|^2 \left| \sum_{j=0}^{n} \beta_j e^{ijka_j} \right|$$

where F is a structure factor, n is the number of graphene layer, f(θ) is an atomic scattering factor which varies from 6.00 to 6.15 e per atom with incident radiation ranging from 2 to 433 keV, $ka_j = (4\pi d_j \sin\theta)/\lambda$, where d_j is a lattice spacing between j^{th} and $(j-1)^{th}$ layer, θ is an angle between the incident ray and the scattering planes, λ is a wavelength of X-ray, and β_j is an occupancy of j^{th} graphene layer. The value of β_j is between 0 and 1.

The three lines in Fig. 8 (dash, dot and dash-dot) are calculated curves from the Equation for $\beta_j \neq 0$, which suggests on distribution of the number of graphene layers. The broadest dash line is calculated curve for uniformly distributed monolayer graphene. The dot line is narrower than the monolayer graphene line, but the broader than the experimental curve (solid line), is calculated curve for a non uniform distribution of graphene layers number for a 3-layered graphene. The dash-dot line is calculated curve for a non uniform distribution of graphene layers number for a multi-layered graphene, whose discrepancy with the experimental curve is due to its asymmetry. However, it provides an increased insight into n-layer graphene regions share, and the results are in agreement with the result obtained by other methods. According to the dash-dot line β_j parameters, the coverages of n-layer graphene regions are calculated as is shown in Table 5.

Table 5: Determined Number of Graphene Layer its Distribution

	Sample 4	Sample 10
Monolayer region coverage	40%	30-35%
3-4 layers region coverage	10%	5-10%
5-6 layers region coverage	15%	5-10%
7-10 layers region coverage	5%	5-10%
> 10 layers region coverage	< 10%	< 10%

The dominant structure of sample 4 is few-layered graphene, and the average value for number of graphene layers is calculated as n = 2.57 for the dominant graphene structure and n = 4.25 for the overall graphene structure. For sample 10, the dominant structure is few-layered, and the average value for number of graphene layers is calculated as n = 3.53 for the dominant graphene structure and n = 5.6 for the overall graphene structure.

4. Conclusions

The research presented in this paper was motivated by the idea to develop a low cost method for high-yield production of graphene. Electrolysis in sulfuric acid electrolyte with reverse change of potential was used. Produced graphene samples were characterized by means of SEM, TEM, TGA/DTG, ATR-FTIR and XRD method. According to the presented results, the following conclusions can be drawn:

- According to the SEM analysis, the graphene samples produced at reverse voltage of 10 to –10 V are characterized with large particle containing lot of defects formed during the exfoliation process, while the samples produced at reverse voltage of +15 to -15 V have shown better morphology and transparency.

- According to TEM analysis, the graphene produced by the electrolysis in sulfuric acid solutions has shown similar morphology to graphene produced by other techniques. The studied samples contain defects as broken and intertwined graphene sheets. The estimated thickness of the produced graphene alters from few nanometers to near 20 nm.

- TGA and DTG have registered several mass

decreases. Since the thermal stability of the obtained graphene decreases as their thickness decreases, TGA results suggest that the samples produced from the graphite M2 have lower thickness (samples 10, 11 and 12) compared to those produced from graphite M1.

- Using FTIR-ATR spectroscopy, characteristic spectra of the studied graphene samples were found: a sharply pronounced peak at 772 cm–1 due to the C–C bond vibrations, as well as some changes of peaks shape in the region of lower wave numbers (400-525 cm–1). This suggests on C–S bonds originated from sulfuric acid and sulfuric atoms present in the medium in which graphene was produced.

- Crystalline structure analysis was completed with X-ray data. Precise determination of the number of graphene layers was done using Laue functions and a model which includes graphene thickness distribution. It was obtained that the dominant structure of sample 4 is few-layered graphene, and the average value for number of graphene layers is calculated as n = 2.57 for the dominant graphene structure and n = 4.25 for the overall graphene structure. For sample 10, the dominant structure is few-layered, and the average value for number of graphene layers is calculated as n = 3.53 for the dominant graphene structure and n = 5.6 for the overall graphene structure.

Acknowledgement

This research was funded by the European Commission through the FP7 Project "Cost-effective sensors, interoperable with international existing ocean observing systems, to meet eu policies requirements" (Project reference 614155) and the Project “Research and development of new nanostructured sensors aimed for protection and development of environment and nature” financed by Ministry of environment and physical planning of R. Macedonia.

References

1. Novoselov KS et al. (2005) Two-dimensional atomic crystals, Proceedings of National Academy of Science. USA 102: 10451-10453.

2. Novoselov KS et al. (2005) Two-dimensional gas of massless Dirac fermions in grapheme. Nature 438: 197-200.

3. Yan L, Zheng YB, Zhao F, et al. (2012) Chemistry and physics of a single atomic layer: strategies and challenges for functionalization of graphene and graphene-based materials. Chem Soc Rev 41: 97-114.

4. Lee J, Tao L, Hao Y, et al. (2012) Embedded-gate graphene transistors for high-mobility detachable flexible nanoelectronics. Appl Phys Lett 100: 152104-152107.

5. Neto AC, Gvineja F, Peres NM, et al. (2009) The electronic properties of grapheme. Review of modern physics 81: 110-117.

6. E. Pop, V. Varshney, A.K. Roy (2012) Thermal properties of graphene: Fundamentals and applications. MRS Bulletin 37: 1273-1281.

7. Sheehy DE, Schmalian J (2009) Optical transparency of graphene as determined by the fine-structure constant. Phys Rev B 80: 193411.

8. Liu Y, Xie B, Zhang Z, et al. (2012) Mechanical properties of graphene papers. J Mecha Phys Solids 60: 591-605.

9. Stoller MD, Park S, Zhu Y, et al. (2008) Graphene-Based Ultracapacitors. Nano Letters 8: 3498-3502.

10. Yang X, Liu G, Balandin AA, et al. (2010) Triple-Mode Single-Transistor Graphene Amplifier and Its Applications. ACS NANO 4: 5532-5538.

11. Bonaccorso F, Sun Z, Hasan T et al. (2010) Graphene photonics and optoelectronics. Nature Photonics 4: 611-622.

12. Vivekchand SRC, Sekhar RC, Subrahmanyam KS (2008) Graphene-based electrochemical supercapacitors. J Chem Sci 120: 9-13.

13. Roy-Mayhew JD, Bozym DJ, Punckt C, et al. (2010) Functionalized graphene as a catalytic counter electrode in dye-sensitized solar cells. ACS NANO 4: 6023-6211.

14. Xu Y, Guo Zh, Chen H, et al. (2011) In-plane and tunneling pressure sensors based on graphene/hexagonal boron nitride heterostructures. Appl Phys Let 99.

15. Petrovski A, Paunović P, Avolio R, et al. (2016) Synthesis and characterization of nanocomposites based on PANI and carbon nanostructures prepared by electropolymerization. Mater Chem Phys 185: 83-90.

16. J. Chen, M. Duan, G. Chen (2012) Continuous mechanical exfoliation of graphene sheets via three-roll mill. J Mater Chem 22: 19625-19628.

17. Zhang Y, Zhang L, Zhou C (2013) Review of Chemical Vapor Deposition of Graphene and Related Applications. Accounts of chemical research 46: 2329-2339.

18. Dreyer DR, Park S, Bielawski CW, et al. (2010) The chemistry of graphene oxide. Chem Soc Rev 39: 228-240.

19. Hernandez Y, Nicolosi Y. Lotya M, et al. (2008) High-yield production of graphene by liquid-phase exfoliation of graphite. Nat Nanotech 3: 563-568.

20. Yua XZ, Hwang CG, Jozwiak CM, et al. (2011) New synthesis method for the growth of epitaxial graphene. J Electron Spectrosc Relat Phenom 184: 100-106.

21. Low CTJ, Walsh FC, Chakrabarti MH, et al. (2013) Electrochemical approaches to the production of graphene flakes and their potential applications. Carbon 54:1-21.

22. Basirun WJ, Sookhakian M, Baradaran S, et al. (2013) Solid-phase electrochemical reduction of graphene oxide films in alkaline solution. Nanoscale Research Letters 8: 397.

23. Wang G, Wang B, Park J, et al. (2009) Highly efficient and large-scale synthesis of graphene by electrolytic exfoliation. Carbon 47: 3242-3246.

24. Alanyahoğlu M, Segura JJ, Oró-Solè J, et al. (2012) The synthesis of graphene sheets with controlled thickness and order using surfactant-assisted electrochemical processes. Carbon 50: 142-152.

25. Liu N, Luo F, Wu H, et al. (2008) One-Step Ionic-Liquid-Assisted Electrochemical Synthesis of Ionic-Liquid-Functionalized Graphene Sheets Directly from Graphite. Adv Funct Mater 18: 1518-1525.

26. Su CY, Lu AY, Xu FR, et al. (2011) High-quality thin graphene films from fast electrochemical exfoliation. ACS Nano 5: 2332-2339.

27. Schnyder B, Alliata D, Kötz R, et al. (2001) Electro chemical intercalation of perchlorate ions in HOPG: an SFM/LFM and XPS study. Appl Surface Sci 173: 221-232.

28. Petrovski A, Dimitrov A, Grozdanov A, et al. (2015) (eds) Nanoscience Advances in CBRN Agents Detection, Information and Energy Security, NATO Science for Peace and Security Series A: Chemistry and Biology.

29. Yanwu Z, Shanthi M, Weiwei C, et al. (2010) Graphene and graphene oxide: synthesis, properties, and applications. Advanced materials 22: 3906-3924.

30. Sun L, Yu H, Fugetsu B (2012) Graphene oxide adsorption enhanced by in situ reduction with sodium hydrosulfite to remove acridine orange from aqueous solution. J Hazard Mate 203/204: 101-110.

31. Mishra AK, Ramaprabhy S (2010) Study of CO2 adsorption in low cost graphite nanoplatelets. Int J of Chem Eng and Appl 1: 266-269.

32. Si Y, Samulski ET (2008) Synthesis of water soluble graphene. Nano Lett 8: 1679-1682.

33. Ueta A, Tanimura Y, Prezhdo OV (2012) Infrared Spectral Signatures of Multilayered Surface-Fluorinated Graphene: A Molecular Dynamics Study. J Phys Chem 116: 8343-8347.

34. Ramana GV, Padya B, Srikanth VS, et al. (2011) Electrically conductive carbon nanopipe-graphite nanosheet/polyaniline composites. Carbon 49: 5239-5245.

35. Ruammaitree A, Nakahara H, Akimoto K, et al. (2013) Determination of non-uniform graphene thickness on SiC (0 0 0 1) by X-ray diffraction. Applied Surface Science 282: 297- 301.

36. Andonovic B, Ademi A, Grozdanov A, et al. (2015) Enhanced model for determining the number of graphene layers and their distribution from X-ray diffraction data. Beilstein J Nanotechnol 6: 2113-2122.

Citation: Anita Grozdanov (2017) Study of Graphene Obtained by Electrolysis in Sulfuric Acid Electrolytes. SF Nanotec Res Let 1:2.